



Published in final edited form as:

Nat Chem Biol. 2012 October ; 8(10): 831–838. doi:10.1038/nchembio.1059.

Ceramide targets autophagosomes to mitochondria and induces lethal mitophagy

R. David Sentelle^{1,2,#}, Can E. Senkal^{1,2,#}, Wenhui Jiang^{1,2}, Suriyan Ponnusamy^{1,2}, Salih Gencer^{1,2}, Shanmugam Panneer Selvam^{1,2}, Venkat K. Ramshesh^{2,3}, Yuri K. Peterson^{2,3}, John J. Lemasters^{2,3}, Zdzislaw M. Szulc^{1,2}, Jacek Bielawski^{1,2}, and Besim Ogretmen^{1,2,*}

¹Departments of Biochemistry and Molecular Biology, Medical University of South Carolina, 86 Jonathan Lucas Street, Charleston, SC, 29425, USA

²Hollings Cancer Center, Medical University of South Carolina, 86 Jonathan Lucas Street, Charleston, SC, 29425, USA

³Department of Pharmaceutical Sciences, Medical University of South Carolina, 86 Jonathan Lucas Street, Charleston, SC, 29425, USA

Abstract

Mechanisms by which autophagy promotes cell survival or death are unclear. We provide evidence that C₁₈-pyridinium ceramide (C₁₈-Pyr-Cer) treatment, or endogenous C₁₈-ceramide generation by ceramide synthase 1 (CerS1) expression mediates autophagic cell death, independent of apoptosis in human cancer cells. C₁₈-ceramide-induced lethal autophagy was regulated via microtubule-associated protein 1 light chain 3 beta lipidation (LC3B-II) and selective targeting of mitochondria by LC3B-II-containing autophagolysosomes (mitophagy) through direct interaction between ceramide and LC3B-II upon Drp1-dependent mitochondrial fission, leading to inhibition of mitochondrial function and oxygen consumption. Accordingly, expression of mutant LC3B with impaired ceramide binding, as predicted by molecular modeling, prevented CerS1-mediated mitochondrial targeting, recovering oxygen consumption. Moreover, knockdown of CerS1 abrogated sodium selenite-induced mitophagy, and stable LC3B knockdown protected against CerS1-C₁₈-ceramide-dependent mitophagy and blocked tumor suppression *in vivo*. Thus, these data suggest a novel receptor function of ceramide for anchoring LC3B-II-autophagolysosomes to mitochondrial membranes, defining a key mechanism for the induction of lethal mitophagy.

Users may view, print, copy, download and text and data- mine the content in such documents, for the purposes of academic research, subject always to the full Conditions of use: http://www.nature.com/authors/editorial_policies/license.html#terms

*To whom correspondence should be addressed: ogretmen@musc.edu; Fax: 843-792-2556.

#These authors contributed equally to this project

Author Contributions: R.D.S performed mitophagy analyses, cell death/OCR measurements, and xenograft studies; C.E.S performed ceramide-LC3B-II binding assays and confocal microscopy; W.J. performed confocal microscopy and OCR measurements; S.P. measured LC3B lipidation; S.G. measured cellular ATP levels; S.P.S measured LC3B lipidation in MEFs; V.K.R performed immunofluorescence and confocal microscopy; Y.K.P performed the structural analysis and docking simulations; J.J.L designed experiments for detection of mitophagy by confocal microscopy and analyzed data; Z.S. designed and synthesized ceramide analogues; J.B. measured ceramides using lipidomics; and B.O. conceived/designed experiments, analyzed data, and wrote the manuscript.

Competing Financial Interests: The authors declare no competing financial interests.

Autophagy is a self-digestion process of cytoplasmic components, such as damaged mitochondria, by double-membrane autophagosomes^{1,2}. In mammals, Atg8 homologue LC3B-I is conjugated with phosphatidylethanolamine (PE), forming LC3B-II and resulting in the maturation of autophagosomes, which associate with lysosomes to form autophagolysosomes³. Autophagy promotes cell survival during starvation⁴ or it can progress to cell death⁵ (lethal autophagy). However, the mechanisms by which autophagy promotes or inhibits cell survival are unclear. Therefore, we sought to resolve this autophagy paradox by defining mechanisms involved in lethal autophagy induction.

Ceramide is a bioactive sphingolipid that mediates cell death^{6,7}. Recently, mammalian ceramide synthases 1-6 (CerS1-6) have been discovered⁸, which regulate the *de novo* generation of ceramides with specific fatty acid chain lengths⁸. For example, CerS1 and CerS6 preferentially generate C₁₈- and C₁₆-ceramide, respectively^{9,10}. CerS1-6-generated ceramides play distinct biological roles¹¹⁻¹³, and CerS1/C₁₈-ceramide has emerged as tumor suppressor in preclinical and clinical studies¹⁴⁻¹⁶.

Although a role for ceramide and other sphingolipids in autophagy induction has been reported¹⁷⁻¹⁹, mechanisms of ceramide signaling in the regulation of lethal autophagy have not been described. Here, we show that C₁₈-ceramide induces lethal autophagy via selective targeting of mitochondria by LC3B-II-containing autophagolysosomes (mitophagy) through direct interaction between ceramide and LC3B-II on mitochondrial membranes. The interaction is regulated downstream of Drp1-mediated mitochondrial fission, leading to caspase-independent cell death. Accordingly, CerS1/C₁₈-ceramide was necessary and sufficient for induction of lethal mitophagy and tumor suppression *in vivo*. Thus, these data provide a mechanistic link between ceramide signaling and lethal autophagy, defining a key component of the survival versus lethal autophagy paradox.

Results

C₁₈-ceramide mediates autophagy-induced cell death

To define whether C₁₈-ceramide regulates survival or lethal autophagy, multiple HNSCC cell lines were treated with a ceramide analogue, containing a pyridinium tether in the C₁₈-sphingosine backbone, D-e-¹⁴C₁₈-pyridinium ceramide bromide (C₁₈-Pyr-Cer; Fig. 1a), which accumulates in mitochondria due to the positive charge localized within the pyridinium ring^{20,21}. The role of C₁₈-Pyr-Cer in inducing LC3B-lipidation (LC3B-II) in the absence or presence of a pancaspase inhibitor Z-VAD or the formation of autophagosomes was determined using western blotting and transmission electron microscopy (TEM), respectively. C₁₈-Pyr-Cer (10 μM, 24 hr) induced LC3B-II formation in UM-SCC-22A cells, and Z-VAD had no effect on this process compared to vehicle-treated controls (Fig. 1b), suggesting a caspase-independent autophagy induction. C₁₈-Pyr-Cer-mediated autophagy in UM-SCC-22A cells was also visualized by TEM, which showed that ceramide treatment increased the formation of autophagosomes compared to controls (Fig. 1c). Moreover, C₁₈-Pyr-Cer mediated LC3B-II formation in multiple other HNSCC cell lines (SCC-1, SCC-22b, OSCC-3, or SCC-24b, and SCC-11b) compared to controls (Supplementary Results, Supplementary Fig. 1a).

To define the role of C₁₈-Pyr-Cer-induced autophagy in mediating cell survival or death, we knocked down autophagy-related genes ATG3 and ATG7 and determined their effects on cell death. Atg3 and Atg7 knockdown using siRNAs (Supplementary Fig. 1b), prevented cell death in response to C₁₈-Pyr-Cer compared to non-targeting scrambled (Scr) siRNA-transfected controls (Fig. 1d). Moreover, C₁₈-Pyr-Cer induced LC3B-II formation in wild-type (wt), but not in ATG5^{-/-} mouse embryonic fibroblasts (MEFs) compared to controls (Supplementary Fig. 1c). Importantly, the loss of *Atg5*, which prevented LC3B-lipidation, protected ATG5^{-/-} MEFs from C₁₈-Pyr-Cer-induced cell death compared to wt controls (Fig. 1e). Then, we examined whether C₁₈-Pyr-Cer mediates cell death in *Bax/Bak*^{-/-23} and caspase 3/7^{-/-24} double knockout (dko) MEFs compared to controls. C₁₈-Pyr-Cer induced death similarly in wt, *Bax/Bak*^{-/-} and caspase 3/7^{-/-} dko MEFs compared to wt (*Bax*^{+/+}/*Bak*^{+/+}) and caspase 3^{+/+}/*caspase*7^{+/+} controls (Fig. 1f). Thus, these data suggest that C₁₈-Pyr-Cer mediates caspase-independent cell death via inducing lethal autophagy.

C₁₈-ceramide targets autophagolysosomes to mitochondria

Because cationic Pyr-Cer analogues accumulate preferentially in mitochondria^{20,21}, we determined whether C₁₈-Pyr-Cer induces mitophagy. First, potential co-localization between mitochondria and autophagolysosomes was visualized by confocal microscopy using UM-SCC-22A and UM-SCC-22B cells stained with MitoTracker Green (MTG), which covalently binds polarized mitochondrial matrix proteins, and LysoTracker Red (LTR), which detects autophagolysosomes^{25,26}. C₁₈-Pyr-Cer induced targeting of mitochondria by autophagolysosomes; MTG and LTR co-localization (yellow) was detected compared to controls, indicating the induction of mitophagy (Fig. 2a and Supplementary Fig. 1d-e). Next, we examined whether targeting mitochondria by C₁₈-Pyr-Cer also alters mitochondrial function using the SeaHorse XF24 to measure the oxygen consumption rate (OCR). C₁₈-Pyr-Cer (1-4 h) reduced the oxygen consumption rate (Supplementary Fig. 2a) compared to controls, indicating mitochondrial dysfunction. Treatment of UM-SCC-22A cells with an inactive dihydro-ceramide analogue, C₁₈-dihydro-Cer-14-piperidine, (Fig. 2b) was not efficient in inducing mitophagy (Supplementary Fig. 2b) or inhibiting OCR (Fig. 2b) when compared to C₁₈-Pyr-Cer. It should be noted that C₁₈-dihydro-Cer-14-piperidine slightly increased MTG/LTR co-localization (Supplementary Fig. 2b) and decreased OCR (Fig. 2b) compared to vehicle treated controls, possibly due to its desaturation to generate active Pyr-Cer in these cells. Moreover, inhibition of lysosomal function using bafilomycin (10 nM) had no effect on the co-localization of MTG and LTR in response to C₁₈-Pyr-Cer (Supplementary Fig. 2c). Thus, these data suggest that C₁₈-ceramide induced targeting of mitochondria by autophagolysosomes (mitophagy)²⁶, consistent with the inhibition of mitochondrial function without altering lysosomal flux.

Endogenous CerS1/C₁₈-ceramide mediates lethal mitophagy

We then examined the roles of endogenously generated C₁₈-ceramide by tetracycline (tet) induction of wt-CerS1-V5 versus the catalytically inactive mutant-CerS1-V5 (His183Ala²⁷), confirmed by western blotting (Fig. 3a), in the regulation of ceramide generation, LC3B-II formation and mitochondrial function in UM-SCC-22A cells. Endogenous ceramide measurement using LC/MS/MS showed that induction of wt-CerS1-V5 selectively increased the generation of C₁₈-ceramide, but not C₁₂-C₂₆-ceramides, compared to non-induced

controls, whereas expression of the catalytically inactive mutant of CerS1 had no effect on C₁₈-ceramide generation (Fig. 3b). Accordingly, CerS1/C₁₈-ceramide induction (+tet) but not the mutant CerS1 resulted in LC3B-II formation, as detected by increased endogenous LC3B-II (Fig. 3a) and LC3B-GFP punctate formation²⁸ (Fig. 3c) compared to controls. Moreover, wt-CerS1 but not the His138Ala-CerS1 decreased OCR (Fig. 3d) and increased co-localization of mitochondrial MTG (green) and autophagolysosomal LTR (red) staining (Fig. 3e), indicating mitophagy. Consistent with inducing mitophagy, wt-CerS1 but not the His138Ala-CerS1 reduced ATP generation compared to controls (Fig. 3f). Importantly, shRNA-dependent stable knockdown of LC3B, which abrogated its lipidation compared to Scr-shRNA controls (Supplementary Fig. 2d), prevented ATP reduction in response to wt-CerS1 expression (Fig. 3g). These data suggest a novel role for tumor suppressor CerS1/C₁₈-ceramide²⁹ in inducing lethal mitophagy.

To determine whether CerS1/C₁₈-ceramide induction is necessary for mediating lethal mitophagy, we treated UM-SCC-22A cells with a known lethal mitophagy inducer sodium selenite (SS)³⁰ and examined its effects on LC3B-II formation, mitophagy and mitochondrial function in the presence of Scr or CerS1 siRNAs. Treatment with SS (5 μM, 3 hr), which increased CerS1 mRNA significantly (about 12-fold, p<0.05; Supplementary Fig. 3a), induced LC3B-GFP punctate formation, whereas CerS1 knockdown (Supplementary Fig. 3b) almost completely prevented LC3B-II formation in response to SS compared to Scr-siRNA transfected cells (Supplementary Fig. 3c). Moreover, SS increased mitophagy at 3-5 h, as detected by co-localization of MTG and LTR staining compared to controls (Supplementary Fig. 3d). Accordingly, SS significantly decreased OCR (about 80%, p<0.05) compared to controls, whereas CerS1 knockdown abrogated the inhibition of OCR by SS (Supplementary Fig. 3e). These data indicate that endogenous CerS1/C₁₈-ceramide plays a key role in SS-mediated mitophagy.

CerS1/C₁₈-ceramide induces LC3B-II-ceramide interaction

Next, we investigated whether CerS1-induced ceramide is localized in mitochondria or ER by confocal microscopy using anti-ceramide³¹ (Enzo Life Sciences) and anti-Tom20 or anti-calreticulin antibodies, respectively. Interestingly, CerS1-induced ceramide in UM-SCC-22A cells was almost exclusively localized within mitochondrial outer membrane (Fig. 4a) but not in the ER (Supplementary Fig. 4a). We also assessed whether CerS1-induced mitochondrial ceramide was co-localized with the CFP-LC3B on mitochondrial membranes by confocal microscopy using anti-ceramide (green), anti-CFP (blue) and MTR (red). Remarkably, CerS1 induced the co-localization of ceramide, LC3B and MTR, with an apparent increase in the formation of white punctates, compared to non-induced controls (Fig. 4b). Mutant-CerS1, which does not generate C₁₈-ceramide, did not result in the co-localization of ceramide-LC3B-mitochondria compared to controls (Fig. 4c). Thus, these data suggest that CerS1-induced ceramide stress mediates co-localization of endogenous ceramide and LC3B-II within mitochondria, consistent with lethal mitophagy.

To explore the role for mitochondrial localization of ceramide in inducing mitophagy, we treated UM-SCC-22A cells with C₁₆-Pyr-Cer, which is also known to mainly accumulate in mitochondria, and measured its effects on mitochondrial function compared to an inactive

analogue, dihydro-C₁₆-Pyr-Cer (Supplementary Fig. 4b). C₁₆-Pyr-Cer inhibited mitochondrial function compared to controls, whereas inactive dihydro-C₁₆-Pyr-Cer did not efficiently decrease OCR when compared to C₁₆-Pyr-Cer (Supplementary Fig. 4c). The conversion of dihydro-C₁₆-Pyr-Cer to C₁₆-Pyr-Cer by DES was also observed, which slightly decreased mitochondrial function compared to vehicle-treated controls (Supplementary Fig. 4c).

We determined the roles of CerS6 expression, which mainly generates C_{14/16}-ceramides, on mitophagy induction. CerS6 induction had no significant effects on LC3B-II formation, MTG/LTR staining or OCR as compared to non-induced controls (Supplementary Fig. 5a-c). Interestingly, we did not detect any localization of CerS6-generated endogenous ceramides within mitochondria, visualized by confocal microscopy using anti-ceramide and MTG (Supplementary Fig. 5d). These data are consistent with distinct biological functions of CerS6-generated endogenous ceramides in the regulation of ER-Golgi membrane integrity and ER-stress responses²⁹, but not in lethal mitophagy. Overall, these data suggest that mitochondrial localization of ceramide, rather than its fatty acid chain length, plays important roles in mitophagy induction. These data also suggest a selective role for CerS1/C₁₈-ceramide or Pyr-Cer analogues, which accumulate within mitochondria, in the induction of lethal mitophagy.

LC3B-II binds ceramide

We explored the mechanisms by which CerS1/C₁₈-ceramide stress induces mitophagy. Ceramide-protein interaction plays various important metabolic and biological roles, such as ceramide-CERT³² binding in the generation of sphingomyelin, ceramide-KSR³³ binding for kinase regulation or ceramide-I2PP2A/SET³⁴ binding for PP2A activation. Therefore, we examined whether LC3B interacts with ceramide. The structure of the ceramide-binding domain of CERT³⁵ suggested that the hydrophobicity and the size of the residues formed within the StART domain play a role in ceramide binding⁴⁸. The globular domain of LC3B³⁶ is structurally similar to the recently solved CERT StART domain^{23,31,35} (Supplementary Fig. 6a). Therefore, we hypothesized that the central globular domain of LC3B, containing Phe52 and Ile35 residues, might be involved in ceramide-binding.

To examine whether CerS1-generated C₁₈-ceramide interacts with LC3B, we labeled UM-SCC-22A cells, stably expressing wt-CerS1, with biotin-sphingosine (B-Sph), which is acylated to form biotin-C₁₈-ceramide upon induction of CerS1. Then, biotin-ceramide-interacting proteins were pulled-down using avidin-conjugated columns, eluted and separated by SDS-PAGE. Interaction of LC3B with ceramide was then examined by western blotting using the anti-LC3B antibody. Data revealed that LC3B-II (14 kDa) but not the non-lipidated LC3B-I binds biotin-C₁₈-ceramide upon CerS1 induction, compared to non-induced or biotin-labeled controls (Supplementary Fig. 6b).

To define whether LC3B-ceramide interaction plays any roles in the regulation of mitophagy, we generated point mutations on residues present in the putative ceramide-binding hydrophobic pocket of LC3B (Supplementary Fig. 7a-b) and examined their effects on ceramide binding, mitophagy and mitochondrial function. Homology modeling, using CERT-ceramide complex structure, revealed the Ile35 and Phe-52 as potential ceramide

binding residues within the hydrophobic pocket of LC3B (Supplementary Fig. 7a-b). Gly120³⁷ is the site for C-terminal lipidation of LC3B with PE³⁷ (Supplementary Fig. 7a and c), which is required for the formation of double-membrane autophagosomal vesicles. Therefore, we expressed wt, Gly120Ala, Ile35Ala or Phe52Ala-LC3B proteins, containing N-terminal FLAG tags in UM-SCC-22A/Tet-CerS1 cells and examined their interaction with endogenous C₁₈-ceramide or C₁₈-Pyr-Cer. The FLAG-wt-LC3B associated with endogenous C₁₈-ceramide and C₁₈-Pyr-Cer (Fig. 5a) compared to controls. In contrast, mutations of the Ile35Ala and Phe52Ala significantly reduced the interaction between LC3B and unlabeled endogenous C₁₈-ceramide (~50 and 90%, p<0.05) or C₁₈-Pyr-Cer (~80 and 95%, p<0.05) compared to that of wt-LC3B (Fig. 5a). Thus, these data suggest that the Ile35 and Phe52 residues of LC3B are involved in C₁₈-ceramide binding.

To determine if LC3B-II selectively binds ceramide based on specific fatty acid chain length, UM-SCC-22A/Tet-CerS1 cells were transfected with wt-LC3B-FLAG and labeled with exogenous ¹⁷C-sphingosine³⁸ (¹⁷C-Sph), containing ¹⁷C-backbone instead of the natural sphingosine with ¹⁸C, which is used as a probe to detect ¹⁷C₁₈-ceramide versus ¹⁷C₁₆-ceramide, respectively (Supplementary Figs. 8 and 9). After immunoprecipitation (IP) using an anti-FLAG antibody in the absence/presence of CerS1 induction (-/+ tet), LC3B-II-FLAG-interacting lipids were extracted, and ¹⁷C-Sph, ¹⁷C-S1P and ¹⁷C₁₂₋₂₆-ceramides were measured. The data showed that LC3B-FLAG strongly associated with CerS1 generated ¹⁷C₁₈-ceramide but not with ¹⁷C_{14-,20-,22}-ceramides or ¹⁷C-S1P in response to CerS1 induction (Supplementary Figs. 8a,b and 9a,b). In addition to endogenous C₁₈-ceramide, LC3B-II also associated with ¹⁷C₁₆-ceramide, ¹⁷C₂₄-ceramide and ¹⁷C-sphingosine in response to CerS1 induction (Supplementary Figs. 8a-c, 9a,b). These data are consistent with the binding preference of CERT, which interacts with multiple ceramide species, such as C₁₆- and C₁₈-ceramides³⁵. Importantly, mutation of LC3B with Ile35Ala or Phe52Ala significantly abrogated endogenously generated ¹⁷C_{18-,16-,24}-ceramide and ¹⁷C-Sph binding (Supplementary Figs. 8a-c, 9a,b). Thus, these data indicate that LC3B binds endogenously generated C₁₈-ceramide as well as C₁₆- and C₂₄-ceramides and sphingosine in response to CerS1 expression.

LC3B lipidation is necessary for ceramide binding

Interestingly, binding of C₁₈-ceramide and C₁₈-Pyr-Cer (Fig. 5a) or ¹⁷C_{18-,16-,24}-ceramides and ¹⁷C-Sph in response to CerS1 induction with the Gly120Ala-LC3B was also decreased compared to wt-LC3B, suggesting that the lipidation of LC3B with PE plays an important role for its binding to ceramide (Fig. 5 and Supplementary Figs. 8,9). This was also consistent with the lack of significant *in vitro* binding between C₁₈-Pyr-Cer and purified wt-LC3B protein, which was not lipidated when expressed in *E-coli* (data not shown).

Accordingly, we determined whether induction of CerS1 influenced the lipidation of wt and mutant forms of LC3B in UM-SCC-22A cells. CerS1/C₁₈-ceramide increased the lipidation of wt-LC3B, forming LC3B-II, but not the Gly120Ala mutant of LC3B compared to non-induced controls (Fig. 5b). Interestingly, mutation of the Ile35Ala or Phe52Ala did not prevent the lipidation of LC3B in response to CerS1/C₁₈-ceramide induction compared to controls (Fig. 5b). Thus, these data suggest that while the lipidation of the Gly120 residue is

important for C₁₈-ceramide interaction, alteration of ceramide binding has no detectable effect on LC3B-II formation.

We then explored the structure of LC3B and ceramide interaction with unmodified and PE modified LC3B in computational docking simulations. Structural analyses suggested that putative binding regions of PE and ceramide are localized on the opposite sites of LC3B (Supplementary Fig. 7a). We therefore created a model of PE modified LC3B to explore potential interactions (Supplementary Fig. 10a,b). Initial analysis of the LC3B structure suggested that it contains a hydrophobic groove that is the most likely site for intramolecular interaction between ceramide/LC3B or PE/LC3B. We then compared the docking of ceramide to unmodified and PE-modified LC3B (Supplementary Fig. 10a,b). The results of the unmodified LC3B docking simulations revealed that among the top 30 poses, none interacted on the face near Phe52, and the vast majority of the docking poses lie in close proximity to Gly120, the PE modification site (Supplementary Fig. 10a). In contrast, docking of ceramide to the PE modified LC3B increased interaction of ceramide at the Phe52 site (Supplementary Fig. 10b). Thus, these data support that PE and ceramide bind on the opposite sites of LC3B, and that LC3B-PE lipidation is important for LC3B-ceramide interaction.

Mitochondrial C₁₈-ceramide-LC3B-II induces mitophagy

We then examined whether ceramide and LC3B-II interaction played any role in targeting or localization of autophagosomes to mitochondria and regulation of mitochondrial function. We ectopically expressed FLAG-tagged wt and mutant LC3B proteins, while endogenous LC3B expression was downregulated using siRNAs that target the 5' untranslated region of LC3B mRNA in UM-SCC-22A/Tet-CerS1 cells. Confocal microscopy revealed that upon expression of the wt-FLAG-LC3B with wt-CerS1 induction, FLAG-LC3B punctuates were formed, which were mainly co-localized with the mitochondrial outer membrane protein Tom20³⁹ compared to non-induced controls (Fig. 6a). However, CerS1/C₁₈-ceramide induction had no effect on the lipidation of the Gly120Ala mutant of LC3B or its localization (Fig. 6a). In addition, the Phe52Ala-LC3B mutant formed puncta, indicating its lipidation, but it did not co-localize with Tom20 in response to wt-CerS1 induction compared to controls (Fig. 6a). Thus, these data suggest that although C₁₈-ceramide interaction is dispensable for the lipidation of LC3B, interaction between ceramide and LC3B plays important roles to target LC3B-II-containing autophagosomes to mitochondria. In addition, CerS1/C₁₈-ceramide decreased OCR in the presence of intact endogenous LC3B expression (in Scr siRNA transfected cells) compared to non-induced controls (Fig. 6b). However, siRNA-mediated knockdown of endogenous LC3B prevented the inhibition of OCR in response to CerS1 induction (Fig. 6b). Remarkably, OCR inhibition was recovered upon reconstitution of the FLAG-wt-LC3B expression after CerS1 induction in response to siRNA-mediated knockdown of endogenous LC3B (Fig. 6b). In contrast, upon downregulation of endogenous LC3B expression using siRNAs, the expression of Phe52Ala-LC3B was not able to recover OCR inhibition in response to CerS1 induction (Fig. 6b). Thus, these data suggest that ceramide and LC3B-II interaction plays key roles in mitochondrial dysfunction upon mitophagy in response to CerS1/C₁₈-ceramide induction.

Ceramide-induced mitophagy requires mitochondrial fission

Because ceramide stress induced LC3B-II/ceramide binding on mitochondrial membranes, it was important to dissect whether mitochondrial fusion and/or fission³⁹ play roles in CerS1/C₁₈-ceramide-mediated mitophagy. Therefore, we examined the effects of genetic loss or siRNA-mediated knockdown of mitofusion-1/2 or Drp1^{39,40}, known regulators of fusion or fission processes, respectively, on ceramide-induced mitophagy. C₁₈-Pyr-Cer inhibited OCR in mitofusion-1/2-/- dko MEFs, similar to wt controls, suggesting that mitochondrial fusion is dispensable in this process (Supplementary Fig. 11a). However, knockdown of Drp1 almost completely prevented ceramide-mediated mitochondrial dysfunction in UM-SCC-22A cells (Fig. 6c). Knockdown of Nix or p62 had no effect on OCR in response to ceramide (Fig. 6c). Consistent with these data, Drp1 knockdown inhibited the targeting of mitochondria by autophagolysosomes in response to C₁₈-Pyr-Cer (Supplementary Fig. 11b). Remarkably, knockdown of Drp1 also attenuated mitochondrial outer membrane localization of ceramide in response to CerS1 induction compared to controls (Fig. 6d and Supplementary Fig. 12a-c). Thus, these data suggest that ceramide-induced mitophagy is regulated downstream of Drp1-mediated mitochondrial fission, whose knockdown alters mitochondrial localization of ceramide on the outer membrane, preventing LC3B-II/ceramide-mediated mitochondrial targeting of autophagolysosomes.

CerS1/C₁₈-ceramide/LC3B axis mediate tumor suppression

We determined whether LC3B-II-mediated autophagy played any role in the regulation of CerS1/C₁₈-ceramide-dependent tumor suppression. First, endogenous LC3B expression was stably knocked down using shRNA expression in UM-SCC-22A/Tet-CerS1 cells, which prevented CerS1-mediated LC3B-II formation compared to controls (Supplementary Fig. 2d). Importantly, stable knockdown of LC3B also prevented inhibition of OCR in response to CerS1 induction (Fig. 7a). Accordingly, CerS1/C₁₈-ceramide significantly inhibited UM-SCC-22A/Tet-CerS1 xenograft-generated tumors (~6-fold, p<0.01) compared to non-induced controls (Fig. 7b). However, shRNA-mediated knockdown of LC3B expression abrogated tumor suppression in response to CerS1/C₁₈-ceramide induction (Fig. 7b). It was also noted that in the absence of ceramide stress, LC3B-mediated autophagy seemed to promote tumor survival and growth, and knockdown of LC3B reduced tumor growth (Fig. 7b). In contrast, LC3B knockdown was protective against CerS1/ceramide-mediated tumor suppression (Fig. 7b). Thus, these data suggest a biological role for LC3B and mitophagy in the regulation of CerS1/C₁₈-ceramide-dependent tumor suppression *in vivo*.

Discussion

In this study, we investigated the roles and mechanisms involved in the regulation of autophagy paradox by ceramide stress. Our data suggest that CerS1/C₁₈-ceramide selectively mediates lethal autophagy, which is Bax/Bak- and caspase-independent, by inducing mitophagy. We discovered that CerS1/C₁₈-ceramide or C₁₈-Pyr-Cer induces LC3B-PE lipidation, forming LC3B-II, which then binds ceramide on the mitochondrial membrane upon Drp1-mediated mitochondrial fission, targeting autophagolysosomes to mitochondria and leading to lethal mitophagy and tumor suppression (Fig. 7c). We believe

that this is one of the first mechanistic links to explain the autophagy paradox, defining how lethal autophagy is regulated by ceramide signaling.

Autophagy can induce survival or death in the same cell type based on different stress conditions, which is context dependent. For example, H₂O₂ mediates autophagy, which is pro-survival in Bax/Bak DKO MEFs⁴¹, whereas etoposide⁴² induces caspase-independent autophagic cell death in these cells. Our data indicate that C₁₈-ceramide mediates non-apoptotic lethal autophagy, which is Bax/Bak- or caspase-independent.

Sphingolipids are known to induce autophagy, which usually protects cells from death in response to serum starvation or inhibition of nutrient uptake⁴³. In contrast, ceramide mediates autophagy, which results in cell death in response to therapeutic treatments in various human cancer cells⁶. In this study, CerS1 expression, generating mainly C₁₈-ceramide, mediated localization of ceramide on the mitochondrial outer membrane, leading to mitophagy, whereas CerS6 expression, which mainly generates C₁₆-ceramide, had no effect on mitochondrial localization of ceramide or mitophagy. However, C₁₆-Pyr-Cer, which localizes to mitochondria, induced mitophagy. These data suggest that different subcellular localization of endogenous ceramides rather than their fatty acid chain lengths plays a key role in mediating their distinct biological functions. These data are in agreement with a recent study, which showed that mitochondrial membrane accumulation of C₁₆-ceramide regulates Bax translocation to mitochondrial membranes, leading to apoptosis in response to SMase induction or radiation³¹.

Ceramide-LC3B-II interaction appears to involve the central hydrophobic domain of the protein, which was somewhat structurally homologous to the ceramide-binding StART domain of CERT³⁵. The binding selectivity of LC3B was also similar to CERT, which is known to bind C₁₈- and C₁₆-ceramides³⁵. The Ile35 and Phe52 residues localized within this hydrophobic domain of LC3B were identified as important for ceramide binding. Interestingly, our data also indicated that PE-conjugation (lipidation) of LC3B also influences ceramide-LC3B-II interaction, because binding of the Gly120Ala-LC3B (non-lipidated mutant) to ceramide was reduced compared to wt protein. Structural analysis and computational simulations indicated that the putative PE and ceramide interaction sites within LC3B might be on opposite faces of the protein, and that PE might mask a low affinity potential ceramide binding site, shifting binding kinetics to the Phe52 site. This hypothesis, however, needs to be further evaluated. Moreover, ceramide induced LC3B lipidation, which was independent of ceramide-LC3B binding. Previous studies suggested that ceramide inhibits protein kinase B, upregulates Beclin¹⁷, and disrupts Bcl-2-Beclin association via JNK1-dependent Bcl-2 phosphorylation¹⁸, leading to Beclin-dependent LC3B lipidation and autophagy¹⁷. However, mechanisms by which ceramide signaling induces LC3B lipidation in HNSCC cells remain unknown.

Interestingly, knockdown of Drp1, which is a known inducer of mitochondrial fission^{39,40}, prevented mitophagy and inhibited mitochondrial membrane localization of ceramide in response to CerS1 expression. Thus, these data suggest that ceramide-mediated mitophagy, which requires LC3B-II formation and ceramide-LC3B-II binding on mitochondrial membranes, is regulated downstream of Drp1-mediated mitochondrial fission. Drp1-

mediated mitochondrial fission is known to induce LC3B lipidation and mitophagy, which requires Parkin/Pink1 or Bnip3 function^{39,40-42,45}. However, the involvement of ceramide as one of the factors that targets LC3B-II-containing autophagolysosomes to mitochondria via ceramide/LC3B-II interaction upon Drp1-induced fission is new.

Overall, these data define at least one key component of the autophagy paradox: LC3B-II-autophagosomes targeting to mitochondrial membranes via C₁₈-ceramide-LC3B-II interaction regulates lethal mitophagy. These data should help to clarify the role of ceramide as a possible receptor for mitochondrial targeting of LC3B-II/autophagosomes, which is linked to HNSCC tumor suppression in response to induction of CerS1/C₁₈-ceramide. These data, by uncovering at least one specific mechanism of how tumor suppressor function of CerS1/C₁₈-ceramide is regulated via lethal mitophagy, might impact the development of therapeutics against various human cancers.

Methods

Ultra structure analysis by TEM

Cells grown in the absence/presence of C₁₈-Pyr-Cer or tet for induction of CerS1 expression were fixed in 2% glutaraldehyde in 0.1M cacodylate following removal of culture medium. After post-fixation in 2% osmium tetroxide, specimens were embedded in epon 812, and sections were cut orthogonally to the cell monolayer with a diamond knife. Thin sections were visualized in a JEOL 1010 transmission electron microscope, as described²⁵.

Laser scanning confocal microscopy

Cultured cells were incubated with 500 nM of MTG or MTR in DMSO for 30 min at 37 °C for covalent labeling of the mitochondria, as described^{25,26,44}. Co-localization of LTR with mitochondria was assessed from fluorescent confocal images of green-fluorescing MTG and red-fluorescing LTR using a 63 × N.A. 1.4 planapochromat oil immersion lens with pinholes set to 1.0 Airy unit in both the red and green channels. LTR and MTG were excited with 543-nm light from a HeNe laser and 488-nm light from an argon laser, respectively, with laser intensities attenuated to 0.05%. Emitted fluorescence was divided by a 545-nm dichroic reflector and passed through 500–530 nm band-pass and 560 nm long-pass barrier filters to measure green and red fluorescence, respectively^{25,26,45}.

Measurement of OCR

Oxygen consumption rate (OCR) in the absence/presence of tet-induction or Pyr-Cer was measured in 1xDMEM supplemented with 10% FBS and 1% penicillin/streptomycin using a Seahorse XF24 (Seahorse Biosciences) as described by the manufacturer. Respiration was expressed as pmol O₂/min.

Ceramide-LC3B binding assays

Association between ceramide and LC3B (wt and mutants) were performed as we described previously³⁴. In summary, cells grown in the absence/presence of tet for induction of CerS1 or CerS6 expression, were labeled with 10 μM biotin-labeled B-Sph (Avanti) for 6-18 hr to generate the biotin-labeled endogenous ceramides. After that, equal amount of cell lysate

(1-2 mg of total protein) for each sample was applied to avidin column, and ceramide-bound proteins were eluted using 2 mM of biotin solution, and concentrated using Centricon (Sigma) for further analysis by SDS-PAGE. The association of wt- and mutant LC3B-FLAG proteins with endogenous ceramides with/without CerS1 induction, in the absence/presence of ^{17}C -Sph to generate $^{17}\text{C}_{12-26}$ -ceramides³⁸, were measured using LC/MS/MS³⁸ after IP using the anti-FLAG antibody. Inorganic phosphate (Pi) was used as an internal control.

Other methods

See Supplementary Methods online for descriptions of reagents, cell lines and culture conditions, plasmids, siRNA and shRNA transfections, mutagenesis of LC3B, molecular modeling/docking simulations, measurement of ATP generation, assessment of xenograft-driven tumor growth *in vivo*, and statistical analysis.

Supplementary Material

Refer to Web version on PubMed Central for supplementary material.

Acknowledgments

We thank Dr. J.G. Schnellmann for her editorial review. We also thank Dr. D.J. Hazen-Martin and her group (Department of Pathology and Laboratory Medicine, Medical University of South Carolina) for TEM preparations. This work was supported by research grants obtained from the National Institutes of Health (CA088932, DE016572 and CA097165 to BO). The core facilities utilized for animal studies, lipidomics and imaging were constructed using support from NIH (C06 RR015455, 5-P30-DK34987, 1-P50-AA11605, or P30 CA138313).

References

1. Mizushima N, Levine B, Cuervo AM, Klionsky DJ. Autophagy fights disease through cellular self-digestion. *Nature*. 2008; 451:1069–1075. [PubMed: 18305538]
2. Yang Z, Klionsky DJ. Eaten alive: a history of macroautophagy. *Nat Cell Biol*. 2010; 12:814–822. [PubMed: 20811353]
3. Tanida I, Ueno T, Kominami E. Human light chain 3/MAP1LC3B is cleaved at its carboxyl-terminal Met121 to expose Gly120 for lipidation and targeting to autophagosomal membranes. *J Biol Chem*. 2004; 279:47704–10. [PubMed: 15355958]
4. Rabinowitz JD, White E. Autophagy and metabolism. *Science*. 2010; 330:1344–1348. [PubMed: 21127245]
5. Vara D, et al. Anti-tumoral action of cannabinoids on hepatocellular carcinoma: role of AMPK-dependent activation of autophagy. *Cell Death Differ*. 2011; 18:1099–1111. [PubMed: 21475304]
6. Salazar M, et al. Cannabinoid action induces autophagy-mediated cell death through stimulation of ER stress in human glioma cells. *J Clin Invest*. 2009; 119:1359–1372. [PubMed: 19425170]
7. Ogretmen B, Hannun YA. Biologically active sphingolipids in cancer pathogenesis and treatment. *Nat Rev Cancer*. 2004; 4:604–16. [PubMed: 15286740]
8. Pewzner-Jung Y, Ben-Dor S, Futerman AH. When do Lasses (longevity assurance genes) become CerS (ceramide synthases)? Insights into the regulation of ceramide synthesis. *J Biol Chem*. 2006; 281:25001–25005. [PubMed: 16793762]
9. Venkataraman K, et al. Upstream of growth and differentiation factor 1 (uog1), a mammalian homolog of the yeast longevity assurance gene 1 (LAG1), regulates N-stearoyl-sphinganine (C18-(dihydro)ceramide) synthesis in a fumonisins B1-independent manner in mammalian cells. *J Biol Chem*. 2002; 277:35642–35649. [PubMed: 12105227]
10. Mizutani Y, Kihara A, Igarashi Y. LASS3 (longevity assurance homologue 3) is a mainly testis-specific (dihydro)ceramide synthase with relatively broad substrate specificity. *Biochem J*. 2006; 398:531–538. [PubMed: 16753040]

11. Rahmaniyan M, Curley RW Jr, Obeid LM, Hannun YA, Kravka JM. Identification of dihydroceramide desaturase as a direct in vitro target for fenretinide. *J Biol Chem.* 2011; 286:24754–24764. [PubMed: 21543327]
12. Deng X, et al. Ceramide biogenesis is required for radiation-induced apoptosis in the germ line of *C. elegans*. *Science.* 2008; 322:110–115. [PubMed: 18832646]
13. Menuz V, et al. Protection of *C. elegans* from anoxia by HYL-2 ceramide synthase. *Science.* 2009; 324:381–384. [PubMed: 19372430]
14. Karahatay S, et al. Clinical relevance of ceramide metabolism in the pathogenesis of human head and neck squamous cell carcinoma (HNSCC): attenuation of C(18)-ceramide in HNSCC tumors correlates with lymphovascular invasion and nodal metastasis. *Cancer Lett.* 2007; 256:101–111. [PubMed: 17619081]
15. Koybasi S, et al. Defects in cell growth regulation by C18:0-ceramide and longevity assurance gene 1 in human head and neck squamous cell carcinomas. *J Biol Chem.* 2004; 279:44311–44319. [PubMed: 15317812]
16. Saddoughi SA, et al. Results of a Phase II Trial of Gemcitabine plus Doxorubicin in Patients with Recurrent Head and Neck Cancers: Serum C18-ceramide as a Novel Biomarker for Monitoring Response. *Clin Cancer Res.* 2011; 17:6097–6105. [PubMed: 21791630]
17. Scarlatti F, et al. Ceramide-mediated macroautophagy involves inhibition of protein kinase B and up-regulation of beclin 1. *J Biol Chem.* 2004; 279:18384–18391. [PubMed: 14970205]
18. Lépine S, Allegood JC, Park M, Dent P, Milstien S, Spiegel S. Sphingosine-1-phosphate phosphohydrolase-1 regulates ER stress-induced autophagy. *Cell Death Differ.* 2011; 18:350–361. [PubMed: 20798685]
19. Sims K, et al. Kdo2-lipid A, a TLR4-specific agonist, induces de novo sphingolipid biosynthesis in RAW264.7 macrophages, which is essential for induction of autophagy. *J Biol Chem.* 2010; 285:38568–38579. [PubMed: 20876532]
20. Szulc ZM, et al. Tailoring structure-function and targeting properties of ceramides by site-specific cationization. *Bioorg Med Chem.* 2006; 14:7083–7104. [PubMed: 16919460]
21. Senkal CE, et al. Potent antitumor activity of a novel cationic pyridinium-ceramide alone or in combination with gemcitabine against human head and neck squamous cell carcinomas in vitro and in vivo. *J Pharmacol Exp Ther.* 2006; 317:1188–1199. [PubMed: 16510697]
22. Mizushima N, Levine B. Autophagy in mammalian development and differentiation. *Nat Cell Biol.* 2010; 12:823–830. [PubMed: 20811354]
23. Lindsten T, et al. The combined functions of proapoptotic Bcl-2 family members bak and bax are essential for normal development of multiple tissues. *Mol Cell.* 2000; 6:1389–1399. [PubMed: 11163212]
24. Masud A, et al. Endoplasmic reticulum stress-induced death of mouse embryonic fibroblasts requires the intrinsic pathway of apoptosis. *J Biol Chem.* 2007; 282:14132–14139. [PubMed: 17371867]
25. Rodriguez-Enriquez S, Kim I, Currin RT, Lemasters JJ. Tracker dyes to probe mitochondrial autophagy (mitophagy) in rat hepatocytes. *Autophagy.* 2006; 2:39–46. [PubMed: 16874071]
26. Kim I, Lemasters JJ. Mitochondrial degradation by autophagy (mitophagy) in GFP-LC3 transgenic hepatocytes during nutrient deprivation. *Am J Physiol Cell Physiol.* 2011; 300:C308–317. [PubMed: 21106691]
27. Spassieva S, et al. Necessary role for the Lag1p motif in (dihydro)ceramide synthase activity. *J Biol Chem.* 2006; 281:33931–33938. [PubMed: 16951403]
28. Shimizu S, et al. Role of Bcl-2 family proteins in a non-apoptotic programmed cell death dependent on autophagy genes. *Nat Cell Biol.* 2004; 6:1221–1228. [PubMed: 15558033]
29. Senkal CE, Ponnusamy S, Bielawski J, Hannun YA, Ogretmen B. Antiapoptotic roles of ceramide-synthase-6-generated C16-ceramide via selective regulation of the ATF6/CHOP arm of ER-stress-response pathways. *FASEB J.* 2010; 24:296–308. [PubMed: 19723703]
30. Kim EH, Choi KS. A critical role of superoxide anion in selenite-induced mitophagic cell death. *Autophagy.* 2008; 4:76–78. [PubMed: 17952022]
31. Lee H, et al. Mitochondrial Ceramide-Rich Macrod domains Functionalize Bax upon Irradiation. *PLoS One.* 2011; 6:e19783. [PubMed: 21695182]

32. Hanada K, et al. Molecular machinery for non-vesicular trafficking of ceramide. *Nature*. 2003; 426:803–809. [PubMed: 14685229]
33. Zhang Y, et al. Kinase suppressor of Ras is ceramide-activated protein kinase. *Cell*. 1997; 89:63–72. [PubMed: 9094715]
34. Mukhopadhyay A, et al. Direct interaction between the inhibitor 2 and ceramide via sphingolipid-protein binding is involved in the regulation of protein phosphatase 2A activity and signaling. *FASEB J*. 2009; 23:751–763. [PubMed: 19028839]
35. Kudo N, et al. Structural basis for specific lipid recognition by CERT responsible for nonvesicular trafficking of ceramide. *Proc Natl Acad Sci U S A*. 2008; 105:488–493. [PubMed: 18184806]
36. Satoo K, et al. The structure of Atg4B-LC3 complex reveals the mechanism of LC3 processing and delipidation during autophagy. *EMBO J*. 2009; 28:1341–1350. [PubMed: 19322194]
37. Ichimura Y, et al. In vivo and in vitro reconstitution of Atg8 conjugation essential for autophagy. *J Biol Chem*. 2004; 279:40584–40592. [PubMed: 15277523]
38. Spassieva S, Bielawski J, Anelli V, Obeid LM. Combination of C(17) sphingoid base homologues and mass spectrometry analysis as a new approach to study sphingolipid metabolism. *Methods Enzymol*. 2007; 434:233–241. [PubMed: 17954250]
39. Youle RJ, Narendra DP. Mechanisms of mitophagy. *Nat Rev Mol Cell Biol*. 2011; 12:9–14. [PubMed: 21179058]
40. Mizushima N, Komatsu M. Autophagy: Renovation of cells and tissues. *Cell*. 2011; 147:728–741. [PubMed: 22078875]
41. Huang Q, Wu YT, Tan HL, Ong CN, Shen HM. A novel function of poly(ADP-ribose) polymerase-1 in modulation of autophagy and necrosis under oxidative stress. *Cell Death Differ*. 2009; 16:264–277. [PubMed: 18974775]
42. Shimizu S, et al. Role of Bcl-2 family proteins in a non-apoptotic programmed cell death dependent on autophagy genes. *Nat Cell Biol*. 2004; 6:1221–1228. [PubMed: 15558033]
43. Guenther GG, et al. Ceramide starves cells to death by downregulating nutrient transporter proteins. *Proc Natl Acad Sci U S A*. 2008; 105:17402–17407. [PubMed: 18981422]
44. Lavieu G, et al. Regulation of autophagy by sphingosine kinase 1 and its role in cell survival during nutrient starvation. *J Biol Chem*. 2006; 281:8518–8527. [PubMed: 16415355]
45. Rikka S, et al. Bnip3 impairs mitochondrial bioenergetics and stimulates mitochondrial turnover. *Cell Death Differ*. 2011; 18:721–731. [PubMed: 21278801]

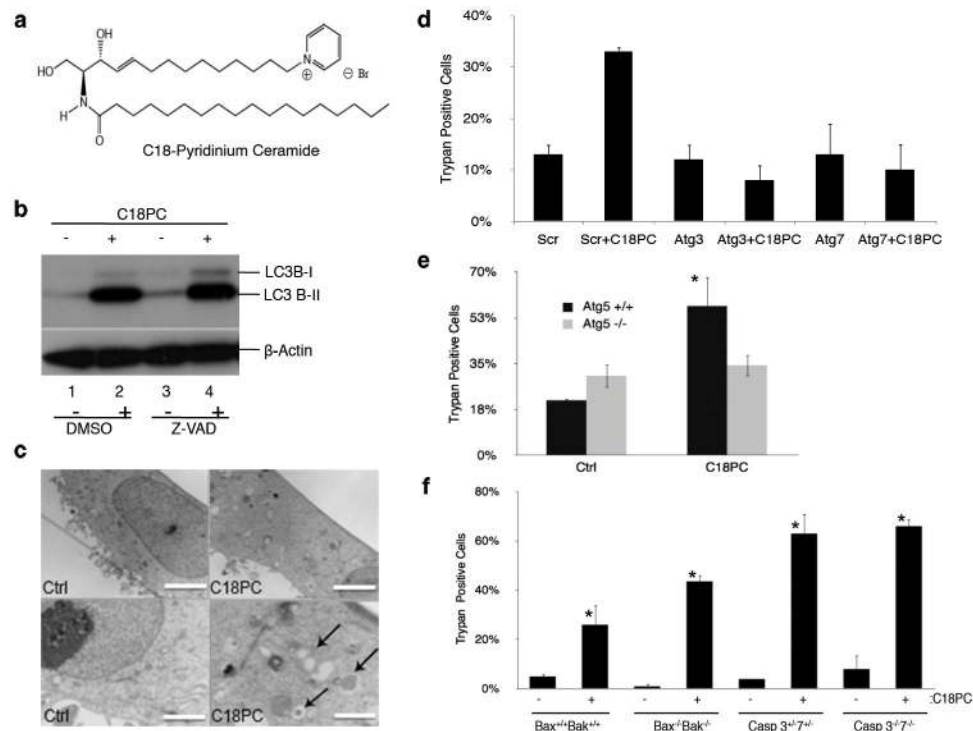


Figure 1. Exogenous C₁₈-Pyr-Cer (C18PC) induces autophagic cell death. **(a)** C₁₈-Pyr-Cer. **(b)** Effects of C₁₈-Pyr-Cer on the lipidation of LC3B (LC3B-II) were examined by western blot in the absence or presence of a pan caspase inhibitor Z-VAD compared to vehicle-treated controls (lanes 1-2 and 3-4, respectively). Full blots can be found in Supplementary Figure 13. **(c)** Formation of double-membrane autophagosomal vesicles in the absence or presence of C₁₈-Pyr-Cer was visualized by TEM (left and right panels, respectively). Higher magnification of TEM visualization is shown in lower panels. Scale bars represent 10 microns (top) and 500 nm (bottom). **(d)** Effects of siRNA-mediated knockdown of Atg3 or Atg7 on cell death in the absence or presence of C₁₈-Pyr-Cer were determined compared to controls transfected with Scr siRNAs using trypan blue exclusion assay. **(e)** Roles of C₁₈-Pyr-Cer in the regulation of lethal autophagy were assessed after treatment of MEFs isolated from wt (ATG5^{+/+}) versus ATG5^{-/-} k/o mice with C₁₈-Pyr-Cer. **(f)** Effects of C₁₈-Pyr-Cer on caspase-dependent or -independent cell death were determined in MEFs isolated from Bax^{-/-}/Bak^{-/-} (dko) or caspase3^{-/-}/7^{-/-} (dko) mice compared to cells isolated from wt (Bax^{+/+}/Bak^{+/+}) or caspase3^{+/-}/7^{+/-} mice, used as controls. Data shown are an average of at least three experiments ± s.d. (**P* < 0.05).

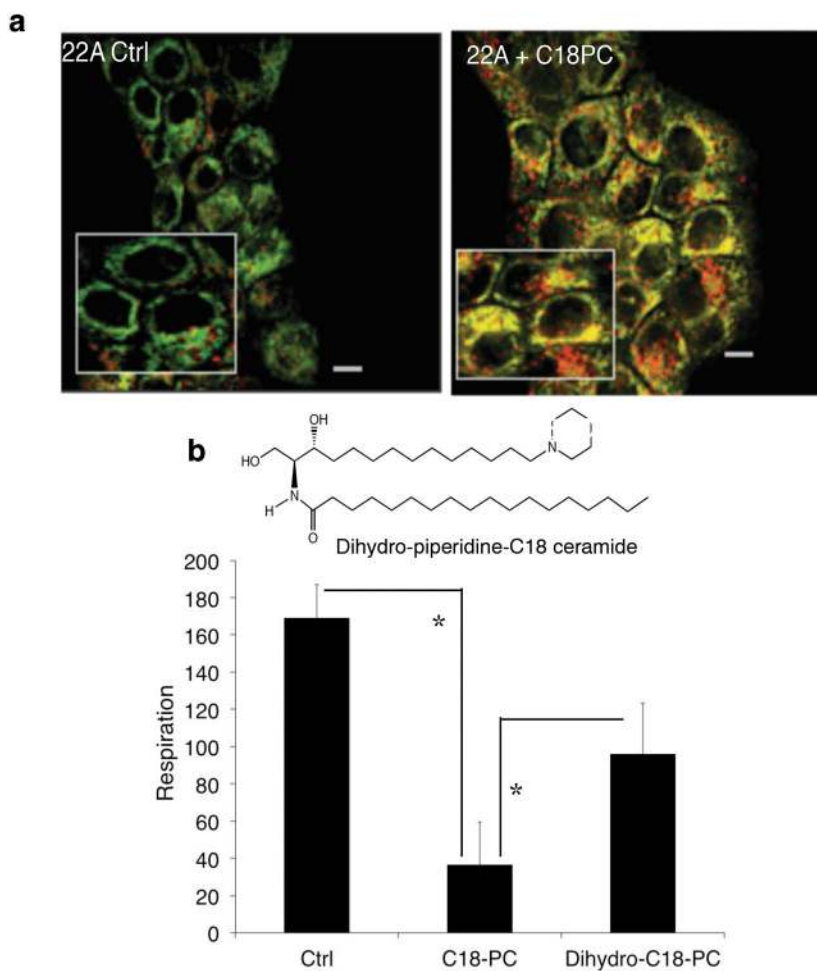


Figure 2. C_{18} -Pyr-Cer mediates targeting of autophagolysosomes to mitochondria and the inhibition of mitochondrial function. **(a)** Targeting of autophagolysosomes to mitochondria in the absence or presence of C_{18} -Pyr-Cer (C18PC) at 2 h in UM-SCC22A cells was examined by visualizing the co-localization of MTG and LTR using live cell imaging and confocal microscopy. Scale bars represent 10 microns. **(b)** Effects of C_{18} -dihydro-Cer-14-piperidine (Dihydro-C18PC, left panel) on OCR were measured using the SeaHorse compared to C_{18} -Pyr-Cer (C18PC) and vehicle-treated controls (right panel). Data shown are an average of at least two independent experiments performed in duplicates \pm s.d. (* $P < 0.05$).

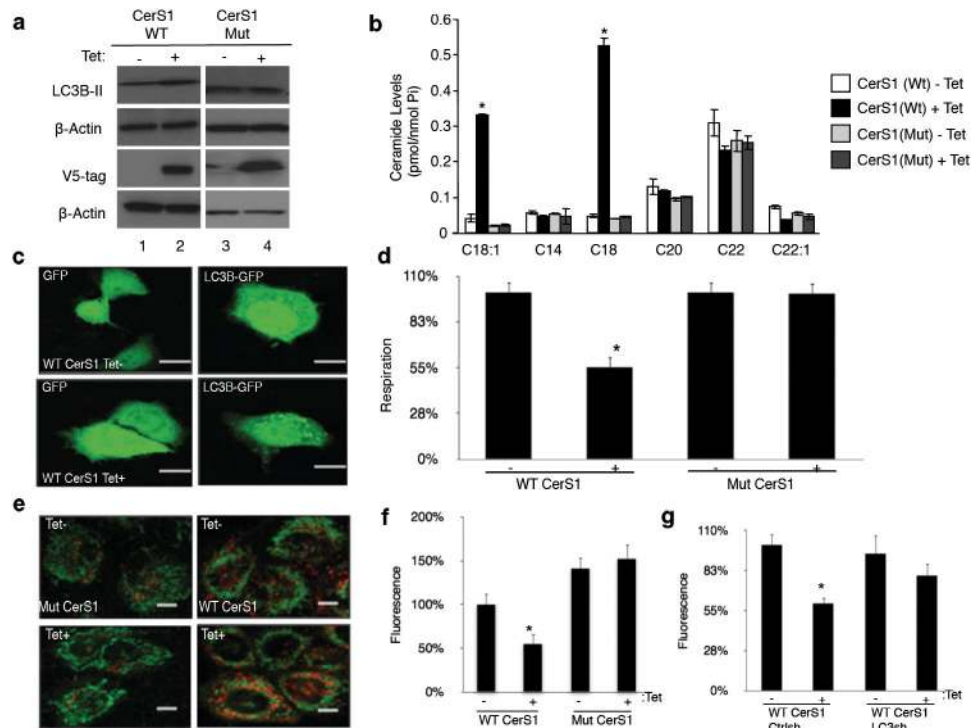


Figure 3. Induction of endogenous C_{18} -ceramide by CerS1 expression mediates lethal mitophagy. **(a)** Effects of induction of wt-CerS1 versus its catalytically inactive mutant, which cannot generate C_{18} -ceramide, expression (containing V5 tags) on the formation of LC3B-II were determined by western blot (first panel, +/-tet, respectively). Successful induction of wt- and mutant-CerS1 expression was confirmed using the anti-V5 antibody. Beta-actin was used as a loading control. Full blots can be found in Supplementary Figure 13. **(b)** Generation of endogenous C_{18} - and $C_{18:1}$ -ceramides in response to wt-CerS1 compared to the mutant-CerS1 induction was measured by LC/MS/MS. **(c)** Effects of wt-CerS1/ C_{18} -ceramide induction (+tet) on GFP or LC3B-GFP lipidation were visualized using confocal microscopy compared to non-induced controls (-tet). Scale bars represent 10 microns. **(d)** Roles of wt-CerS1/ C_{18} -ceramide versus the catalytically inactive mutant-CerS1 induction (+tet) in the regulation of mitochondrial function was assessed by measuring oxygen consumption rate using the SeaHorse, compared to non-induced controls (-tet). **(e)** Targeting mitochondria with autophagolysosomes in the absence or presence of wt-CerS1/ C_{18} -ceramide (-/+ tet, respectively) was visualized by co-localization of MTG and LTR using confocal microscopy. **(f)** Effects of wt and mutant CerS1 (-/+ tet) on ATP generation. Scale bars represent 10 microns. **(g)** Effects of wt-CerS1 (-/+ tet) on ATP generation in the absence or presence of shRNA-mediated knockdown of LC3B were measured. Data shown are an average of at least three experiments \pm s.d. (* $P < 0.05$).

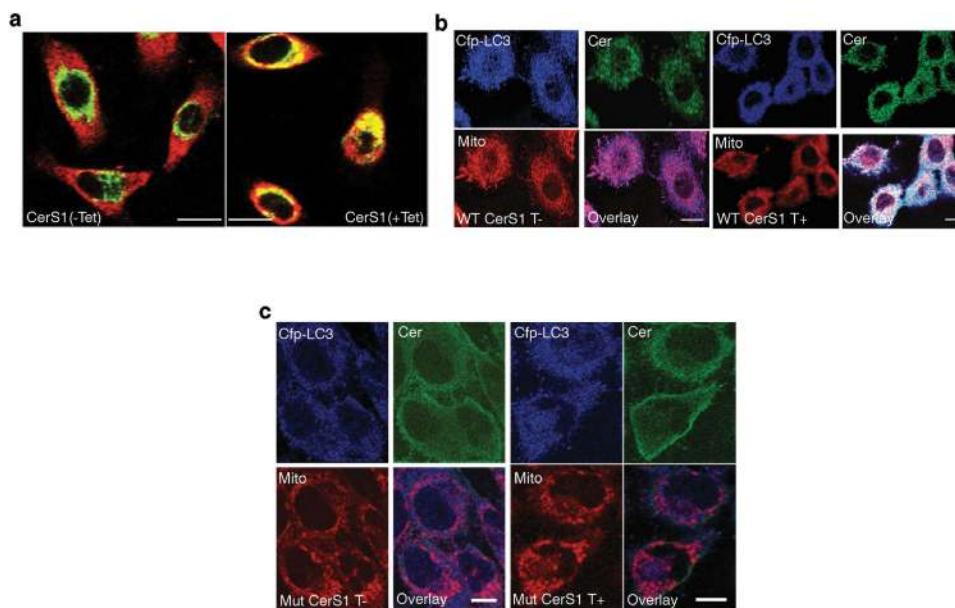


Figure 4. Mitochondrial localization of CerS1-generated C_{18} -ceramide induces targeting of mitochondria by LC3B-II-containing autophagosomes. **(a)** Subcellular localization of ceramide, generated by wt-CerS1 induction (+tet), in mitochondria were visualized by colocalization of ceramides and mitochondria using anti-ceramide and anti-Tom-20 antibodies, respectively, using confocal microscopy. **(b-c)** Mitochondrial targeting of LC3B-II and C_{18} -ceramide, generated by induction of wt-CerS1 (b) versus the catalytically inactive mutant CerS1 (c) expression (+tet) was visualized by co-localization of ceramide (green), LC3B-CFP (blue) and MitoTracker Red (MTR) using anti-ceramide antibody and confocal microscopy. Non-induced cells (-tet) were used as controls. Scale bars represent 10 microns.

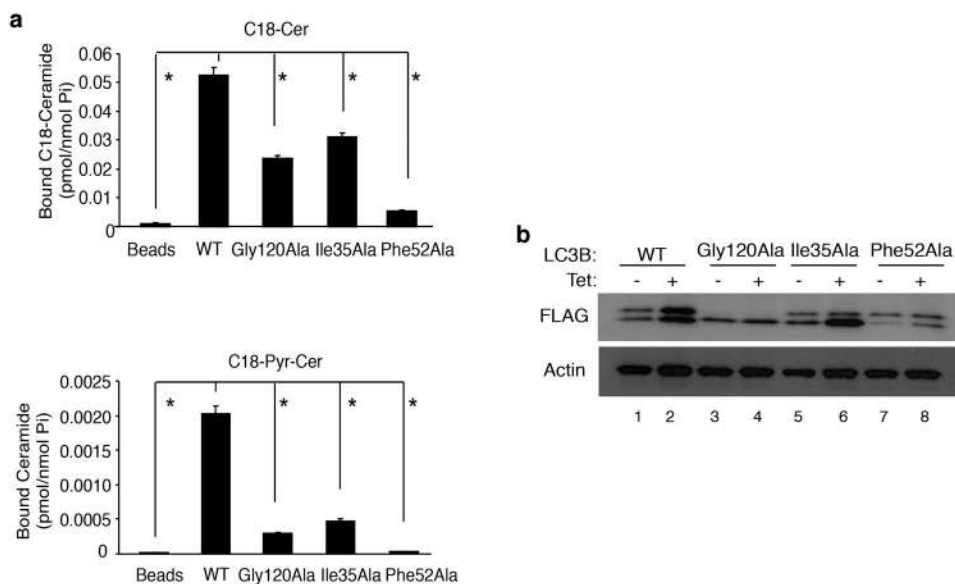
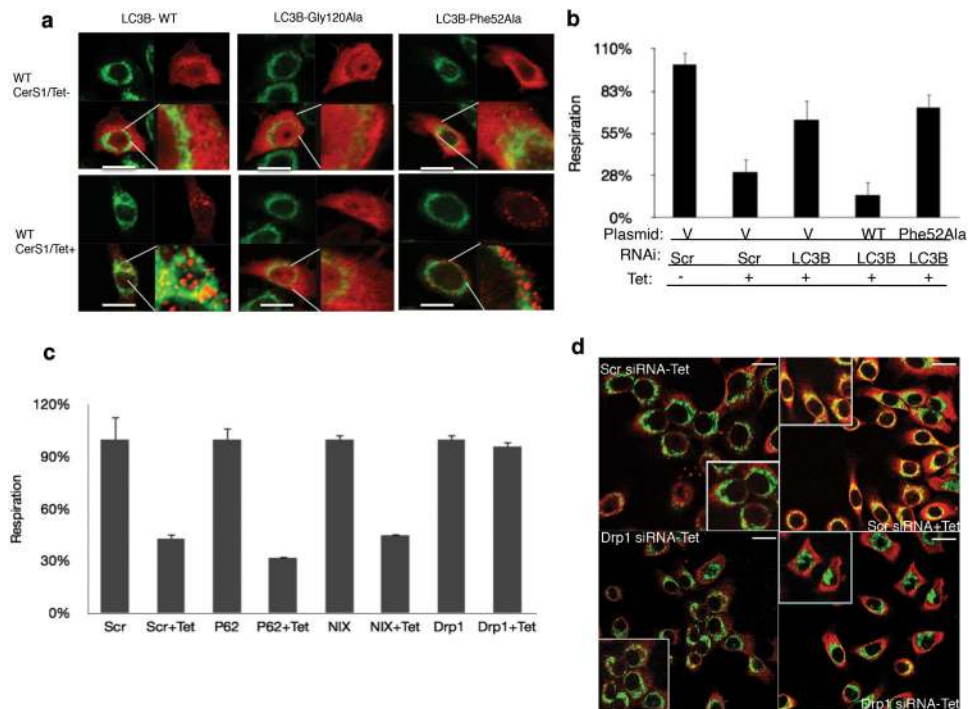


Figure 5. C_{18} -ceramide interacts with LC3B via lipid-protein association. **(a)** Binding of wt-, Ile35Ala-, Phe52Ala- or Gly120Ala-LC3B-FLAG proteins with endogenous C_{18} -ceramide, generated in response to wt-CerS1 induction (upper panel) or exogenous C_{18} -Pyr-Cer (lower panel) were measured using LC/MS/MS after pull-down using anti-FLAG antibody-conjugated beads. Data shown are an average of at least three experiments \pm s.d. ($*P < 0.05$). **(b)** Effects of CerS1/ C_{18} -ceramide induction on the lipidation of wt-, Ile35Ala-, Phe52Ala- or Gly120Ala-LC3B-FLAG proteins were examined by western blot. Non-induced cells (-tet) were used as controls. Beta-actin was used as a loading control. Full blots can be found in Supplementary Figure 13.

**Figure 6.**

C_{18} -ceramide-LC3B-II interaction on mitochondrial membranes is regulated downstream of Drp1-mediated mitochondrial fission. **(a-b)** Effects of Gly120Ala and Phe52Ala conversions, which perturbed C_{18} -ceramide-binding of LC3B, on targeting mitochondria by LC3B-containing autophagosomes (visualized by confocal microscopy using anti-FLAG and anti-Tom-20 antibodies; a) or mitochondrial function (measurement of oxygen consumption OCR; b). **(c)** Roles of siRNA-mediated knockdown of p62, NIX and Drp1 in the alteration of OCR in the absence or presence of CerS1/ C_{18} -ceramide induction (-/+Tet) were measured using the Seahorse. Data shown are an average of at least three experiments \pm s.d. (* $P < 0.05$). **(d)** Effects of siRNA-mediated knockdown of Drp1 on the localization of ceramide within mitochondrial membranes were visualized using the co-localization of anti-ceramide (red) and anti-Tom20 (green) antibodies under confocal microscopy, in the absence or presence of CerS1/ C_{18} -ceramide induction (-/+ Tet) compared to Scr-siRNA-transfected controls (right and left, upper and lower panels, respectively). Scale bars represent 10 microns in (a) and (d).

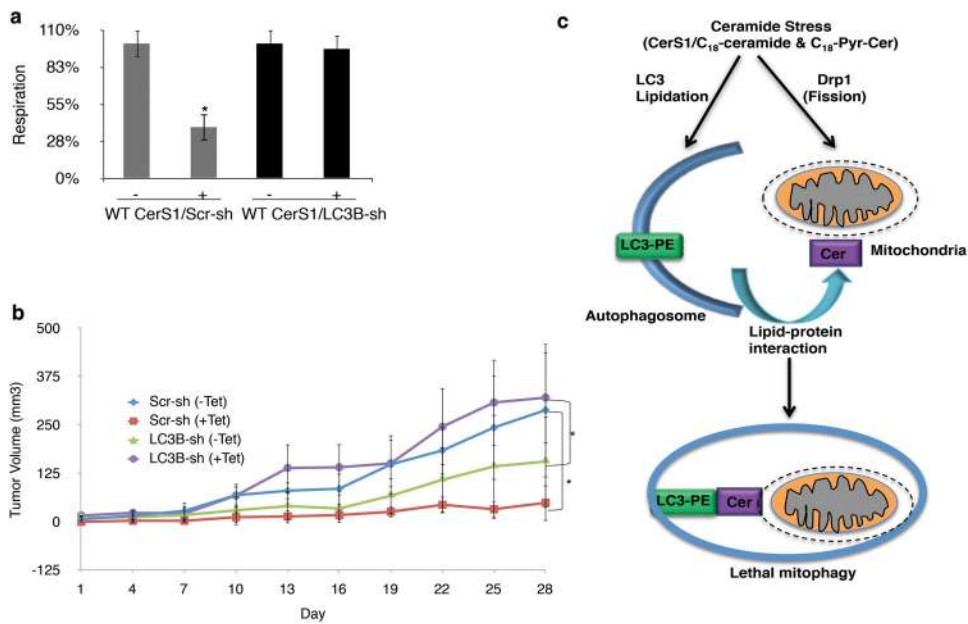


Figure 7. C₁₈-ceramide-LC3B interaction induces lethal mitophagy and subsequent tumor suppression *in vivo*. **(a-b)** Roles of shRNA-mediated stable knockdown of endogenous LC3B expression in the regulation of mitochondrial function (a), or UM-SCC-22A xenograft-derived tumor growth in the absence/presence of wt-CerS1/C₁₈-ceramide induction (-/+ tet) were determined using the SeaHorse, or measurement of tumor volumes in the flanks of SCID mice (n=6/group), respectively. Data shown are an average of at least three experiments ± s.d. (**P* < 0.05). **(c)** Mechanism by which C₁₈-ceramide induces lethal autophagy involves, at least in part, the lipidation of LC3B, forming LC3B-II, and interaction of LC3B-II and ceramide on mitochondrial membranes upon Drp1-mediated mitochondrial fission, which targets autophagosomes to mitochondria for lethal mitophagy.